

Strong Low-Frequency Quantum Correlations From a Four-Wave Mixing Amplifier

C. F. McCormick, A. M. Marino, V. Boyer, and P. D. Lett*

Atomic Physics Division, National Institute of Standards and Technology, Gaithersburg MD 20899 USA

(Dated: September 26, 2018)

We show that a simple scheme based on nondegenerate four-wave mixing in a hot atomic vapor behaves like a near-perfect phase-insensitive optical amplifier, which can generate bright twin beams with a measured quantum noise reduction in the intensity difference of more than 8 dB, close to the best optical parametric amplifiers and oscillators. The absence of a cavity makes the system immune to external perturbations, and the strong quantum noise reduction is observed over a large frequency range.

PACS numbers: 42.50.Gy, 42.50.Dv

Two-mode squeezed beams have become a valuable source of entanglement for quantum communications and quantum information processing [1]. These applications bring specific requirements on the squeezed light sources. For instance, for squeeze light to be used as a quantum information carrier interacting with material system, as in an atomic quantum memory, the light field must be resonant with an atomic transition and spectrally narrow to ensure an efficient coupling between light and matter. In recent years, attention has also been brought to the problem of the manipulation of cold atomic samples with non-classical fields in order to produce non-classical matter waves [2, 3, 4]. In this case, the slow atomic dynamics also requires squeezing at low frequencies.

The standard technique for generating nonclassical light fields is by parametric down-conversion in a crystal, with an optical parametric oscillator or an optical parametric amplifier [5, 6]. While very large amounts of quantum noise reduction have been achieved in this way [7, 8], controlling the frequency and the linewidth of the light remains a challenge. Only recently have sources based on periodically-poled nonlinear crystals been developed at 795 nm to couple to the Rb D1 atomic line [9, 10]. On the other hand, stimulated four-wave mixing (4WM) naturally generates narrow-band light close to an atomic resonance, but its development as an efficient source of squeezed light has been hindered by fundamental limitations such as spontaneous emission. At the end of the 1990s, nondegenerate 4WM in a double-lambda scheme was identified as a possible workaround for these limitations, as described in Ref. [11] and references therein. It was not until recently that such a scheme was implemented in continuous mode in an efficient way in both the low [12, 13, 14] and the high [15, 16] intensity regimes, where it was shown to generate twin beams where quantum correlations are not masked by competing effects.

The double-lambda scheme gives rise to complex atomic dynamics and propagation properties, such as slow-light effects [17]. In this Letter, we show that in spite of this complexity, the quantum properties of the scheme can be accurately described as the combination of a perfect amplifier and a partial absorber. This model

allows us to optimize the quantum noise reduction in the intensity difference of the bright twin beams and to isolate the limiting factors of this reduction. It also helps to identify regions of the parameter space where the system behaves like a perfect phase-insensitive amplifier, opening the way to the generation of strong continuous-variable entanglement. Finally, we demonstrate the intrinsic robustness of our scheme by measuring large levels of squeezing in the audio range, at frequencies where technical noise usually represents a serious obstacle to the generation and the observation of quantum effects.

The double-lambda scheme (Fig. 1a) is a 4WM process which, *via* the interaction with 4 atomic levels, mixes 2 strong pump fields with a weak probe field in order to generate a fourth field called the conjugate. The probe and conjugate fields (the twin beams) are cross-coupled and are jointly amplified, which leads to intensity correlations stronger than the standard quantum limit (SQL). These correlations are the manifestation of two-mode quadrature squeezing between opposite vacuum sidebands of the twin beams.

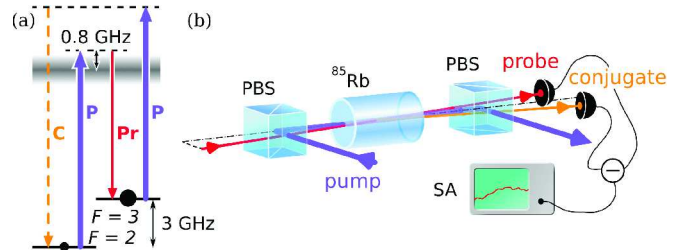


FIG. 1: (color online). Experimental details. (a) Four-level double-lambda scheme in ^{85}Rb , P = pump, C = conjugate, Pr = probe. The width of the excited state represents the Doppler broadened profile. (b) Experimental setup, PBS = polarizing beam splitter, SA = spectrum analyzer.

As in the experiments presented in [16], we use a cw Ti:Sapphire ring laser, to generate a strong (≈ 400 mW) pump beam near the D1 line of Rb (795 nm). From this we derive, using an acousto-optic modulator, a weak (≈ 100 μW) probe beam tuned ≈ 3 GHz to the red of the pump. This results in very good relative phase stability

of the probe with respect to the pump. The pump and probe beams are cross-linearly polarized, combined in a Glan-Taylor polarizer, and directed (at an angle of 0.3 degrees to each other) into a 12.5 mm vapor cell filled with isotopically pure ^{85}Rb (see Fig. 1). The cell, with no magnetic shielding, is heated to $\approx 110^\circ\text{C}$. The windows of the cell are anti-reflection coated on both faces, resulting in a transmission for the probe beam of 98% per window. The pump and probe are collimated with waists at the cell position of $650\ \mu\text{m}$ and $350\ \mu\text{m}$ ($1/e^2$ radius) respectively.

After the cell we separate the pump and probe beams using a second polarizer, with $\approx 10^5 : 1$ extinction ratio for the pump. With the pump at ω_0 , tuned to a ‘one-photon detuning’ of 800 MHz to the blue of the ^{85}Rb $5S_{1/2}F = 2 \rightarrow 5P_{1/2}$, D1 transition, and the probe at ω_- , detuned 3040 MHz to the red of the pump (‘two-photon detuning’ of 4 MHz), we measure an intensity gain on the probe of 9. This gain is accompanied by the generation of the conjugate beam at ω_+ , detuned 3040 MHz to the blue of the pump, which has the same polarization as the probe, and propagates at the pump-probe angle on the other side of the pump so that it fulfills the phase-matching condition. After the second polarizer we direct the probe and conjugate beams into the two ports of a balanced, amplified photodetector. The output of this photodetector is fed into a radio frequency spectrum analyzer with a resolution bandwidth (RBW) of 30 kHz and a video bandwidth (VBW) of 300 Hz. In addition, we introduce a delay line into the conjugate beam path to compensate for the differential slow-light delay discussed in Ref. [17]. This results in a fraction of a dB improvement in the amount of squeezing observed and increases the squeezing bandwidth up to 20 MHz.

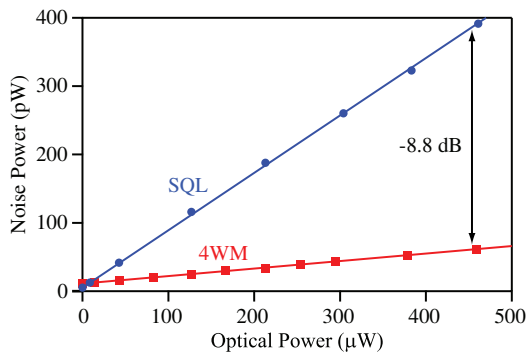


FIG. 2: (color online). Intensity-difference noise versus total optical power at 1 MHz. Circles: SQL; red squares: 4WM. The ratio of the two slopes is -8.8 dB.

We measure -8.0 dB of intensity-difference squeezing at an analysis frequency of 1 MHz without compensating for any system noise. This noise has contributions from the electronic noise of the detection system and the pump light that scatters from the atomic medium. In order to

determine the effect of the system noise on the measured squeezing we vary the input probe power and we plot in Fig. 2 the intensity-difference noise of the probe and conjugate beams versus the total (probe plus conjugate) power incident on the detector, as well as the standard quantum limit (SQL), determined by measuring shot-noise-limited balanced beams of the same total power. The two curves fit to straight lines, with a ratio of slopes equal to $0.131 = -8.8$ dB. The SQL curve has a zero-intercept given by -82.9 dBm, while the zero-intercept of the probe-conjugate curve is higher, -79.6 dBm (due to the pump scattering). The optical path transmission and photodiode efficiencies are $(95.5 \pm 2)\%$ and $(94.5 \pm 2)\%$, respectively, resulting in a total detection efficiency of $\eta = (90 \pm 3)\%$; all uncertainties are estimated 1 standard deviation. The squeezing value at the end of the atomic medium, corrected for losses, is better than -11 dB.

We turn to a simple model of distributed gain and loss in the medium [18, 19] to isolate the few physical concepts necessary to describe the 4WM process and to quantitatively explain the measured squeezing. Two-mode squeezing is produced in an ideal medium of gain G , with negligible absorption, where the photon annihilation operators \hat{a} and \hat{b} for the probe and the conjugate fields transform according to

$$\hat{a} \rightarrow \hat{a}\sqrt{G} - \hat{b}^\dagger\sqrt{G-1} \quad (1)$$

$$\hat{b}^\dagger \rightarrow \hat{b}^\dagger\sqrt{G} - \hat{a}\sqrt{G-1}. \quad (2)$$

When the probe port a is seeded with a coherent state $|\alpha\rangle$ and the conjugate port b is fed with the vacuum, the output intensity-difference noise is equal to the shot noise of $|\alpha\rangle$, which gives a quantum noise reduction of $1/(2G-1)$ with respect to the output SQL.

In our experiment the probe, unlike the conjugate, is tuned close enough to an atomic resonance to experience some absorption [see Fig. 1(a)]. The coherent coupling between probe and pump leads to a certain degree of electromagnetically-induced transparency (EIT) for the probe [11]. Imperfections such as stray magnetic fields, the residual Doppler effect, atomic collisions and short atomic transit time through the beams, as well as the depumping due to the conjugate-pump lambda system limit this effect. In addition, the atomic susceptibility results in an offset of the gain maximum from the EIT absorption minimum [17]. Localized loss in the system can be modeled by a beam splitter of transmission T picking off a fraction of the probe and injecting the vacuum on the second input port (photon annihilation operator \hat{c}), according to the transformation:

$$\hat{a} \rightarrow \hat{a}\sqrt{T} + \hat{c}\sqrt{1-T} \quad (3)$$

$$\hat{b}^\dagger \rightarrow \hat{b}^\dagger. \quad (4)$$

Because of the vacuum noise injected into port c , such a transformation applied to the squeezed probe and con-

jugate is expected to degrade the squeezing. In the actual medium, gain and loss are distributed and can be modeled by a succession of $N \gg 1$ interleaved stages of elementary gain g and N stages of elementary transmission t . The intrinsic gain G (probe transmission T) of the whole stack is obtained by making $t = 1$ ($g = 1$), respectively. Finally, the total detection efficiency η is also modeled by a beam splitter of transmission η applied to both the probe and conjugate fields. In the calculations below we set $N = 200$.

The experimentally accessible parameters are the effective (measured) probe gain of the medium G_{eff} , defined as the probe power out of the cell divided by the probe power in (corrected for window losses), and the ratio r of conjugate-to-probe output powers. Both parameters depend on the intrinsic gain the loss of the probe in the medium. From G_{eff} and r , we use the model to numerically determine G and T without any free parameters. Experimentally, the parameter space is probed by scanning the one-photon detuning from 0.4 to 1.4 GHz. This effectively changes both the gain and the transmission of the probe in a coupled manner. Figure 3 shows the theoretical intensity-difference squeezing obtained from the model described above as well as the measured squeezing (corrected for the system noise) as a function of the probe transmission T , and the gain G . The main result is that, as shown in Fig. 3, the experimental data points agree very well with the simple gain/loss model.

The theoretical surface of Fig. 3 shows that for a given probe transmission there is an optimum gain. At lower gain the intensity-difference squeezing is limited by the power imbalance between the probe and the conjugate, which originates from the input probe power. At larger gain the squeezing becomes limited by the amplification of the noise introduced by the loss on the probe. In the same way, for a given gain there is an optimum transmission value, smaller than 1, corresponding to this trade-off between power balancing and absorption-induced quantum noise. In order to increase the squeezing, it would be necessary to both reduce the probe absorption and increase the gain. Experimentally, the absorption and the gain both depend on the cell temperature (both increase with the atomic density) and the pump detuning, and they are not independently controllable. The best squeezing of -8.8 dB is obtained over the transmission range of 0.85–0.95, and gains of 9–15. This best value can be achieved over a range of several degrees in temperature.

An interesting feature revealed by the data in Fig. 3 is that at large one-photon detunings, the probe transmission becomes unity for an intensity-difference squeezing of about -7 dB. It is therefore possible to operate the system as an ideal amplifier with a gain up to about 6, producing, in principle, a pure entangled state which could be a valuable resource for some quantum information protocols.

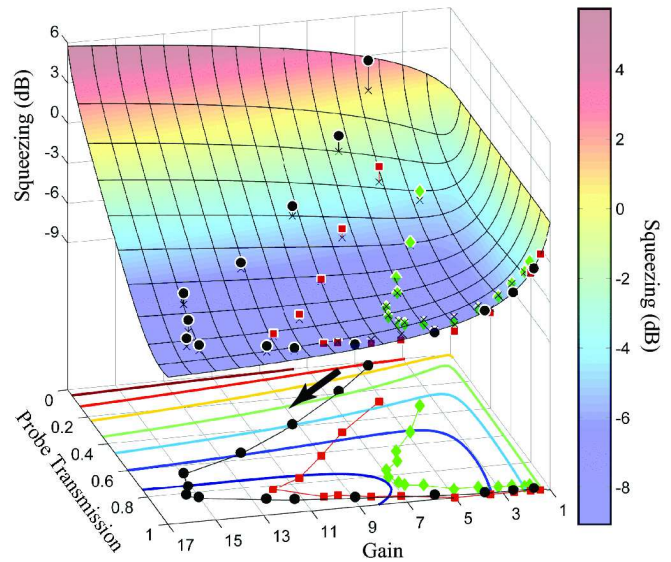


FIG. 3: (color online). Simulated and measured intensity-difference squeezing as a function of the probe transmission T and medium gain G . The theory takes into account the detection efficiency ($\eta = 0.9$). The squeezing (corrected for the system noise) measured at 1 MHz is shown for different cell temperatures, 109°C (diamonds), 112°C (squares), and 114°C (circles), as the one-photon detuning of the pump laser is scanned. The crosses indicate the projection of the measured squeezing onto the theoretical surface while the lines connecting the spheres and crosses give an indication of the vertical distance between them. Most of the points are very near the surface. The projection onto the $x - y$ plane shows contour lines of the theoretical squeezing at 2 dB intervals from $+4$ to -8 dB, and the projections of the data points. The arrow indicates the direction of increasing one-photon detuning.

In addition to looking at the level of noise reduction obtained at a fixed frequency, we can also investigate the frequency spectrum of the noise reduction. Since there is no fundamental limitation on the low-frequency response of the system [11, 17], it will be established by technical noise on the pump and probe lasers. The small number of optical components and particularly the lack of a cavity minimizes the coupling to the environment. To explore this, we record the intensity-difference noise spectrum at low analysis frequencies with the detunings fixed at 800 MHz for the one-photon detuning and 4 MHz for the two-photon detuning. The probe (conjugate) output powers are equal to 305 (290) μW , and the RBW and the VBW are reduced (see Fig. 4). The intensity-difference noise signal is 8.0 dB below the SQL and almost flat, with the exception of a few resonance peaks, all the way down to 4.5 kHz. At this point the technical noise of the pump and probe lasers starts to dominate, resulting in the loss of the intensity-difference squeezing at frequencies below 2.5 kHz. While making these measurements we found

that the frequency stabilization of the Ti:sapphire laser adds amplitude noise to the beam, which in turn prevents squeezing from being observed below 70 kHz. The data in Fig. 4 were taken with the active frequency stabilization of the laser turned off. The observation of squeezing in the kHz range makes our system suitable for applications such as the transfer of optical squeezing onto matter waves [2].

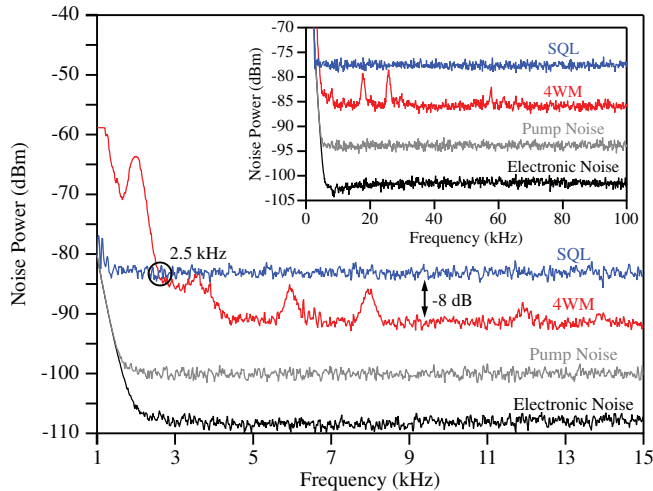


FIG. 4: (color online). Low-frequency squeezing. Noise spectra (RBW=0.3 kHz, VBW=3 Hz) for the electronic noise, the pump scattering, the intensity-difference, and the standard-quantum limit. The inset shows a larger frequency span (RBW=1 kHz, VBW=10 Hz).

In addition to making the system insensitive to environmental noise, the lack of a cavity allows the system to operate as a multi-spatial-mode phase-insensitive amplifier [20], making it an ideal source for quantum imaging experiments [21]. When coupled to the low-frequency squeezing capability of our system, multimode operation could find an interesting application in photothermal spectroscopy, which measures the deflection of a beam at frequencies of the order of 1 kHz, and is currently nearly limited by the shot-noise [22].

An important property of twin beams is the presence of continuous-variable EPR (Einstein-Podolsky-Rosen) entanglement [23]. In its current configuration, in which the probe and conjugate are 6 GHz apart in frequency, the presence of entanglement can be verified through the use of two different local oscillators, or a bichromatic local oscillator [24]. In addition, the reciprocity between the beams involved in the 4WM process should allow the pumping to occur at the two frequencies ω_+ and ω_- , in order to generate frequency degenerate twin beams at frequency ω or to realize a phase-sensitive amplifier.

We have demonstrated a simple and robust source of intensity-difference-squeezed light based on four-wave mixing in a hot atomic vapor capable of producing a

quantum noise reduction in the intensity difference of more than 8 dB over a large frequency range. The system provides a narrowband non-classical source near an atomic transition and is well-suited for use in light-atom interaction experiments. In addition, we have shown that under certain conditions the system behaves as an ideal phase-insensitive amplifier, opening the way to the generation of pure entangled states. This realization of a high-quality source of non-classical light may find a place in a variety of applications.

This work was supported in part by the IC postdoctoral program. We thank Luis Orozco and Ennio Arimondo for helpful discussions.

* Electronic address: paul.lett@nist.gov

- [1] S. L. Braunstein and P. van Loock, *Rev. Mod. Phys.* **77**, 513 (2005).
- [2] S. A. Haine, M. K. Olsen, and J. J. Hope, *Phys. Rev. Lett.* **96**, 133601 (2006).
- [3] P. D. Lett, *J. Mod. Opt.* **51**, 1817 (2004).
- [4] S. A. Haine and J. J. Hope, *Phys. Rev. A* **72**, 033601 (2005).
- [5] A. Heidmann *et al.*, *Phys. Rev. Lett.* **59**, 2555 (1987).
- [6] S. Feng and O. Pfister, *Phys. Rev. Lett.* **92**, 203601 (2004).
- [7] J. Laurat, L. Longchambon, C. Fabre, and T. Coudreau, *Opt. Lett.*, **30**, 1177 (2005).
- [8] H. Vahlbruch *et al.*, *Phys. Rev. Lett.* **100**, 033602 (2008).
- [9] T. Tanimura, D. Akamatsu, Y. Yokoi, A. Furusawa, and M. Kozuma, *Opt. Lett.* **31**, 2344 (2006).
- [10] G. Hétet *et al.*, *J. Phys. B* **40**, 221 (2007).
- [11] M. D. Lukin, P. R. Hemmer, and M. O. Scully, *Adv. At. Mol. Opt. Phys.* **42**, 347 (2000).
- [12] V. Balic, D. A. Braje, P. Kolchin, G. Y. Yin, and S. E. Harris, *Phys. Rev. Lett.* **94**, 183601 (2005).
- [13] P. Kolchin, S. Du, C. Belthangady, G. Y. Yin, and S. E. Harris, *Phys. Rev. Lett.* **97**, 113602 (2006).
- [14] J. K. Thompson, J. Simon, H. Loh, and V. Vuletic, *Science* **313**, 74 (2006).
- [15] C. H. van der Wal *et al.*, *Science* **301**, 196 (2003).
- [16] C. F. McCormick, V. Boyer, E. Arimondo, and P. D. Lett, *Opt. Lett.* **32**, 178 (2007).
- [17] V. Boyer, C. F. McCormick, E. Arimondo, and P. D. Lett, *Phys. Rev. Lett.*, **99**, 143601 (2007).
- [18] J. R. Jeffers, N. Imoto, and R. Loudon, *Phys. Rev. A* **47**, 3346 (1993).
- [19] M. Fiorentino, J. E. Sharping, P. Kumar, and A. Porzio, *Opt. Express* **10**, 128 (2002).
- [20] V. Boyer, A. M. Marino, and P. D. Lett, arXiv:0711.3439 [quant-ph] (2007).
- [21] M. I. Kolobov, ed., “Quantum Imaging” (Springer, New York, 2007).
- [22] M. A. Owens, C. C. Davis, and R. R. Dickerson, *Anal. Chem.* **71**, 1391 (1999).
- [23] M. D. Reid, *Phys. Rev. A* **40**, 913 (1989).
- [24] A. M. Marino *et al.*, *J. Opt. Soc. Am. B*, **24**, 335 (2007).